Magnetic dichroism study of the relativistic electronic structure of perpendicularly magnetized Ni/Cu(001)

W. Kuch, M. Zharnikov, A. Dittschar, K. Meinel, C. M. Schneider, and J. Kirschner
Max-Planck-Institut für Mikrostrukturphysik, Am Weinberg 2, D-06120 Halle, Germany

J. Henk and R. Feder
Theoretische Festkörperphysik, Universität Duisburg, D-47048 Duisburg, Germany

An experimental and theoretical study of magnetic circular dichroism in valence band photoemission from 15 monolayer thick fcc Ni films on Cu(001) is presented. A highly symmetric configuration (light incidence, electron emission, magnetization direction, photon helicity, and surface normal all parallel) allows the illustrative interpretation of the dichroism in terms of the relativistic band structure. Photoemission experiments in the photon energy range of 11–27 eV are compared to fully relativistic one-step photoemission calculations. From this comparison, the dichroic features can be directly related to the double group symmetry of the initial states, which is demonstrated by two examples. © *1996 American Institute of Physics.* [S0021-8979(96)26808-3]

The interplay of spin-orbit and exchange interaction in ferromagnets is of great interest for a variety of effects. Magnetic dichroism in photoemission, which is the change of intensity distribution curves by reversal of the magnetization direction, is exclusively due to this interplay of spin-orbit and exchange interaction.[1] Magnetic circular dichroism in valence-band photoemission (MCDAD), therefore, is an especially well-suited method to study this interaction in the valence states. We want to demonstrate in this contribution that information on the relativistic electronic structure is available by MCDAD which otherwise would have been accessible by spin-resolved photoemission only.

Thin Ni films (10–56 ML), grown epitaxially on Cu(001), have their easy axis of magnetization perpendicular to the film surface.[2] They offer thus the advantage to study the MCDAD in a totally symmetric configuration. Such a configuration, in which the light incidence, electron emission, magnetization direction, and photon helicity are all aligned parallel to the surface normal, allows the illustrative interpretation of the observed dichroism in terms of double-group symmetry of the initial bands along the Δ axis of the relativistic band structure.

We present an experimental and theoretical MCDAD study of the spin-orbit and exchange split electronic structure of fcc-Ni(001) films. Fully relativistic one-step photoemission calculations were performed. We show that from the comparison between experiment and theory it is possible to determine details of the relativistic band structure such as band dispersion and hybridization between bands of the same double group symmetry.

Ni films of 15 ML thickness were deposited at room temperature by electron bombardment of a high-purity nickel rod. The films were annealed immediately after deposition for 10 min at 450 K in order to minimize the film roughness.[3] Photoemission spectra were taken at the Berlin synchrotron radiation facility (BESSY), with $\approx$ 90% circularly polarized light. The overall energetic resolution was approximately 200 meV, the angular acceptance better than $\pm 2°$. The films were remanently magnetized perpendicular to the surface prior to the acquisition of the spectra. All spectra were collected at room temperature.

Fully relativistic one-step photoemission calculations of the layer Korringa–Kohn–Rostoker (KKR) type were performed using a recently developed Green's function formalism.[4] Details of the calculation procedure will be given elsewhere.[5] The spectra were calculated for a semi-infinite Ni(001) crystal with the lateral lattice constant of bulk Cu, namely, 2.55 Å (compared to 2.49 Å for bulk Ni). The vertical layer spacing was taken as 1.69 Å, which means a 6% tetragonally compressed fcc structure. Such a structure is deduced from our LEED $I(V)$ measurements of the specular beam. Furthermore, we assume $T=0$ K and complete polarization of the incident light.

In a highly symmetric arrangement without the presence of a magnetic field, electronic transitions induced by circularly polarized light are governed by relativistic dipole selection rules.[6] In the presence of a perpendicular magnetization, the electronic states can be classified due to four one-dimensional irreducible representations of the double group, which read Δ_6+, Δ_6-, Δ_7+, and Δ_7-. Their Δ^5 spatial parts can be labeled Δ_6^5+, Δ_6^5-, Δ_7^5+, and Δ_7^5-.[5] The $+/-$ sign should not be attributed to majority or minority spin because the latter is not a ''good quantum number'' in the presence of spin-orbit coupling.

Figure 1 illustrates the situation. In the bottom panel, the energetic positions of the four bands are depicted schematically. Transitions from this states induced by circularly polarized light depend on the relative orientation of photon spin $\boldsymbol{\sigma}$ and magnetization $\mathbf{M}$. If $\boldsymbol{\sigma}$ is parallel (antiparallel) to $\mathbf{M}$, only states with Δ_7^5+ and Δ_6^5- (Δ_7^5- and Δ_6^5+) symmetry contribute to the spectrum.[6] In the center panel of Fig. 1, schematic intensity distribution curves for the two cases are shown. The solid (dotted) lines correspond to parallel (antiparallel) alignment of $\boldsymbol{\sigma}$ and $\mathbf{M}$ [$I(\uparrow\uparrow)$ and $I(\uparrow\downarrow)$, respectively)]. The resulting normalized intensity asymmetry, defined as $A=[I(\uparrow\uparrow)-I(\uparrow\downarrow)]/[I(\uparrow\uparrow)+I(\uparrow\downarrow)]$, is depicted in the top panel. It exhibits a characteristic plus/minus/plus feature, where the minus indentation is evoked by emission from the Δ_6^5+ and Δ_7^5- bands.

Figure 2 shows a series of intensity spectra for different photon energies. Following the convention of Fig. 1, spectra

 0021-8979/96/79(8)/6426/3/$10.00

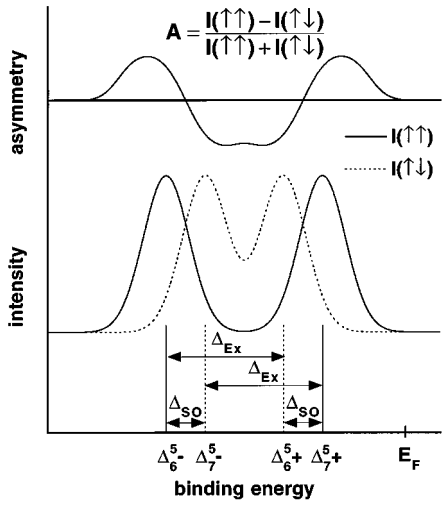

FIG. 1. Bottom: schematic representation of the four bands of Δ_7^5+, Δ_6^5+, Δ_7^5-, and Δ_6^5- symmetry contributing to the spectra in the totally symmetric geometry. The arrows indicate the splitting due to spin-orbit (Δ_{SO}) and exchange interaction (Δ_{Ex}). Center: schematic intensity distribution curves for parallel (solid lines) and antiparallel alignment (dotted lines) of photon spin and magnetization direction. Top: normalized asymmetry A of the spectra of the center panel.

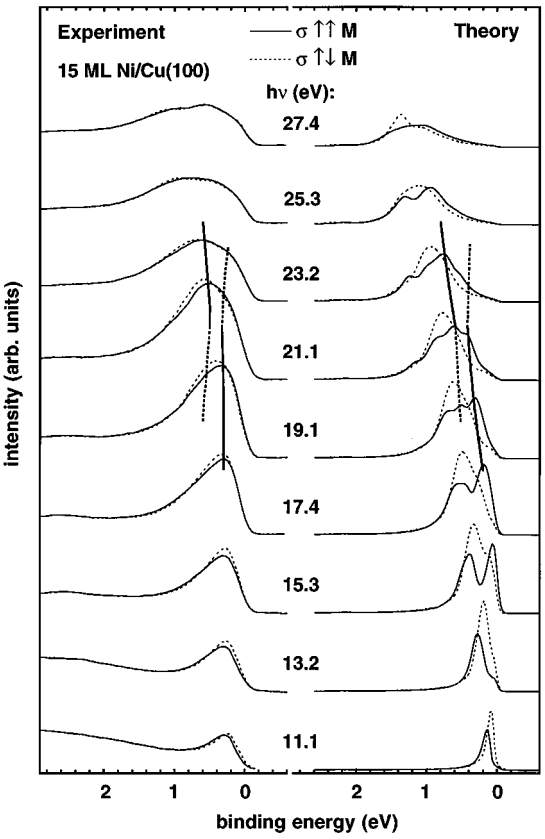

FIG. 2. Series of partial intensity spectra for different photon energies $h\nu$. Shown are spectra for parallel (solid lines) and antiparallel alignment (dotted lines) of photon spin and magnetization direction. Left: experimental spectra, right: theoretical spectra. The vertical lines indicate the occurrence of a hybridization region as explained in the text.

for parallel (antiparallel) alignment of $\boldsymbol{\sigma}$ and $\mathbf{M}$ are reproduced by solid (dotted) lines. Experimental spectra, normalized to the photon flux, are depicted on the left-hand side, the results of the calculation on the right-hand side. The spectra for 11.1 eV photon energy display relatively sharp peaks just below the Fermi energy; with increasing photon energy a dispersion towards higher binding energies and a broadening of the peaks are observed both in the experimental and in the theoretical spectra.

Figure 3 displays asymmetry spectra, corresponding to the intensity spectra of Fig. 2. Again, experimental asymmetries are shown on the left, theoretical curves on the right-hand side. At small photon energies, experimental asymmetries as large as 20% are observed. In order to facilitate comparison with the experimental data, the theoretical asymmetry curves are scaled by a factor of 0.2. The experimental spectra exhibit significantly broader intensity curves and lower asymmetries compared to the calculated ones, which must be attributed to the limited energetic and angular resolution, to possible imperfections in film morphology, and to the background of inelastically scattered electrons not considered in the calculations. Furthermore, the theoretical spectra were calculated for $T=0$ K and 100% circular polarization. A larger broadening of the calculated spectra would lead to a better agreement but impedes the identification of the underlying electronic transitions. Apart from the different size of the dichroic asymmetry, very good qualitative agreement between experiment and theory is seen both in the intensity and in the asymmetry spectra. This enables us to correlate the experimentally observed features to the calculated relativistic band structure.

We will now demonstrate by two examples how this comparison of experiment to theory serves to identify specific details of the electronic states, assuming direct interband transitions. Figure 4 shows the relativistic band structure of Ni along the Δ axis, calculated with the same parameters as the photoemission spectra. The bands are reproduced with differently dashed and dotted lines according to their double group symmetry, as labeled in the figure.

Let us now as the first example consider the dispersion of the four bands with Δ^5 spatial symmetry which were used for the schematic illustration of Fig. 1. In Fig. 4 these bands are marked by four arrows at both sides of the panel. Starting at the Γ point at binding energies between 1.5 and 1.9 eV, these bands jointly disperse upwards, interrupted by hybridization with other bands, to reach the X point at energies between 0.15 eV below and 0.3 eV above the Fermi energy. In the experiment a photon energy of 11 eV corresponds to transitions near the X point, whereas 27 eV corresponds to transitions near the Γ point. Comparing experimental spectra to the calculated band structure, off-axis contributions due to the experimental angular resolution have principally to be considered and may contribute to the linewidth of the spectra. At $\pm 2°$, however, these effects are small and affect mainly the relative peak heights.[7] Because of the broadening of the spectra at higher photon energies, it is difficult to obtain the dispersion of the Δ^5 bands from intensity spectra alone. As we see from Fig. 1, the pronounced minus feature in the asymmetry curves is correlated to the energetic posi-

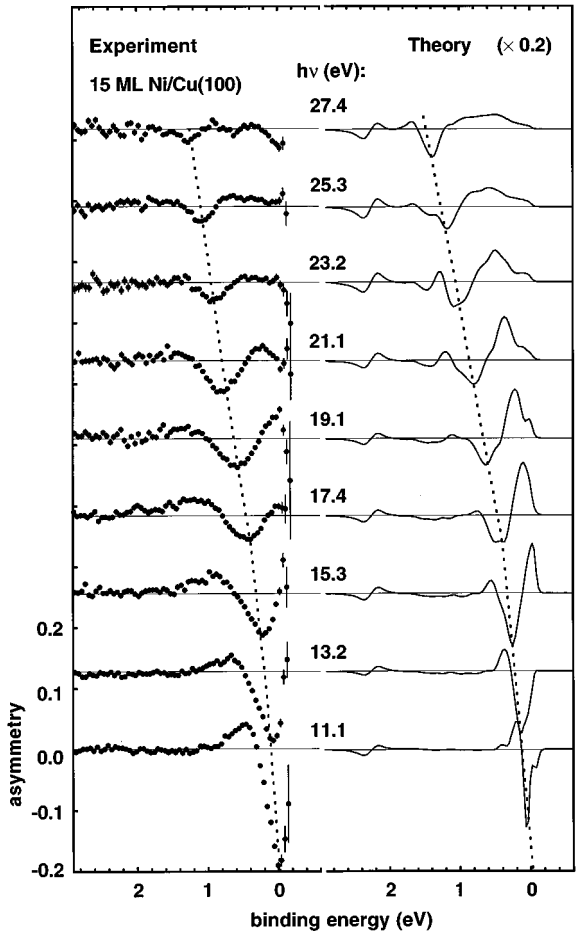

FIG. 3. Series of asymmetry spectra for different photon energies $h\nu$, calculated from the corresponding spectra of Fig. 2. Left: experimental asymmetries, right: theoretical asymmetries. The vertical dotted lines mark the dispersion of the prominent minus peak.

tions of the Δ_6^5+ and Δ_7^5- bands. The dispersion of this minus peak, marked by vertical dotted lines in Fig. 3, indicates the dispersion of the Δ^5 bands.

As a second example we will consider the hybridization of Δ_7+ bands around 0.5 eV binding energy at about the middle of the Δ axis. This hybridization is caused by an avoided crossing between a band of Δ_7^2+ symmetry, which is recognized in Fig. 4 by a weak dispersion, and a band of Δ_7^5+ symmetry with a steeper dispersion. As a consequence of the avoided crossing, the bands interchange their symmetry character in the hybridization region and contain both a mixture of Δ_7^2+ and Δ_7^5+ symmetry. This can be seen in the intensity spectra for $\boldsymbol{\sigma}\uparrow\uparrow\mathbf{M}$ (solid lines in Fig. 2). As already mentioned, only bands which contain Δ^5 single group symmetry character contribute to the spectra. This means that the hybridization is observed as an energetic displacement of the corresponding peak towards higher binding energy with increasing photon energy. The vertical lines in Fig. 2 indicate the region of hybridization in the photoemission spectra.

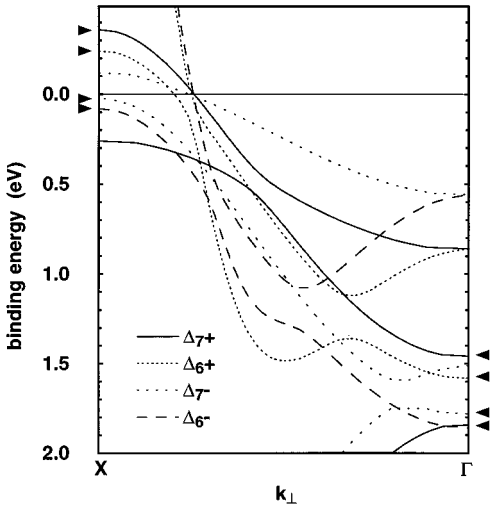

FIG. 4. Relativistic band structure of Ni along the Δ axis, calculated with the same parameters as the photoemission spectra. Bands with Δ_7+, Δ_6+, Δ_7-, and Δ_6- double group symmetry are distinguished as labeled in the figure. The arrows indicate bands of Δ^5 orbital symmetry.

They mark the positions of bands containing Δ_7^5+ symmetry, and fade out into dotted lines where the Δ_7^2+ symmetry character in these bands predominates. In the calculated spectra (right-hand side of Fig. 2), both of the hybridizing bands can be distinguished as separate peaks in the solid line spectra. In the experimental spectra (left-hand side of Fig. 2), the hybridization shows up as energetic shift of the intensity weight of the peak for $\boldsymbol{\sigma}\uparrow\uparrow\mathbf{M}$ between 19.1 and 21.1 eV. Whereas at 19.1 eV the peak is asymmetrically shaped with higher weight at the low binding energy side, at 21.1 eV the weight is shifted to the side with higher binding energy.

Both examples demonstrate how the relativistic band structure can be correlated to MCDAD spectra. It has been shown how from the comparison to fully relativistic calculations even fine details of the band structure can be resolved. This demonstrates the capability of magnetic circular dichroism in valence-band photoemission for the investigation of the exchange and spin-orbit split relativistic band structure of ferromagnets.

Financial support by the BMBF under Grants No. 05-621EFA and 05-5PGABB7 is gratefully acknowledged.

[1] L. Baumgarten, C. M. Schneider, H. Petersen, F. Schäfers, and J. Kirschner, Phys. Rev. Lett. **65**, 492 (1990); B. T. Thole and G. van der Laan, Phys. Rev. B **44**, 12 424 (1991).
[2] F. Huang, M. T. Kief, G. J. Mankey, and R. F. Willis, Phys. Rev. B **49**, 3962 (1994); W. L. O'Brien and B. P. Tonner, *ibid.* **49**, 15370 (1994); B. Schulz and K. Baberschke, *ibid.* **50**, 13467 (1994).
[3] J. Shen, J. Giergiel, and J. Kirschner, Phys. Rev. B **52**, 8454 (1995).
[4] S. V. Halilov, E. Tamura, H. Gollisch, D. Meinert, and R. Feder, J. Phys.: Cond. Matt. **5**, 3859 (1993).
[5] W. Kuch, A. Dittschar, K. Meinel, M. Zharnikov, C. M. Schneider, J. Kirschner, J. Henk, and R. Feder (unpublished).
[6] M. Wöhlecke and G. Borstel, Phys. Rev. B **23**, 980 (1981).
[7] S. V. Halilov, J. Henk, T. Scheunemann, and R. Feder, Phys. Rev. B **52**, 14 235 (1995).